Research in Microbiology 170 (2019) 171–181

Contents lists available at ScienceDirect

Research in Microbiology

journal homepage: www.elsevier.com/locate/resmic

Original Article

The bifunctional protein GlmU is a key factor in biofilm formation induced by alkylating stress in *Mycobacterium smegmatis*

Angela Di Somma [a, 1], Marianna Caterino [b, 1], Vijay Soni [c], Meetu Agarwal [c], Pamela di Pasquale [a], Stefania Zanetti [d], Paola Molicotti [d], Sara Cannas [d], Vinay Kumar Nandicoori [c], Angela Duilio [a, *]

[a] Department of Chemical Sciences, University of Naples 'Federico II', Naples, Italy
[b] Department of Molecular Medicine and Medical Biotechnology, University of Naples "Federico II", Naples, Italy
[c] National Institute of Immunology, International Centre for Genetic Engineering and Biotechnology, Aruna Asaf Ali Marg, New Delhi, 110067, India
[d] Department of Biomedical Science, University of Sassari, Sassari, Italy

ARTICLE INFO

Article history:
Received 9 November 2018
Accepted 21 March 2019
Available online 3 April 2019

Keywords:
DNA alkylation
Comparative proteomics
Biofilm formation
Mycobacterium tuberculosis (MTB)
Bifunctional protein GlmU

ABSTRACT

Living organisms have developed specific defence mechanisms to counteract hostile environmental conditions. Alkylation stress response mechanisms also occur in *Mycobacterium tuberculosis* (MTB) the pathogen responsible for tuberculosis. The effect of alkylating agents on the cellular growth of MTB was investigated using methyl methanesulfonate (MMS) as methyl donor demonstrating that limited doses of alkylating agents might affect MTB cell viability. A global investigation of *Mycobacterium smegmatis* response to alkylating stress was then pursued by differential proteomics to identify the most affected cellular pathways. Quantitative analysis of proteomic profiles demonstrated that most of the proteins upregulated in the presence of alkylating agents are involved in biofilm formation and/or cell wall biosynthesis. Tailored experiments confirmed that under stress conditions *M. smegmatis* elicits physical defence mechanisms by increasing biofilm formation. Among the upregulated proteins, we identified the GlmU bifunctional enzyme as a possible factor involved in biofilm production. Experiments with both conditional deletion and overexpressing *glmU* mutants demonstrated that down regulation of GlmU decreased *M. smegmatis* capabilities to produce biofilm whereas overexpression of the enzyme increased biofilm formation. These results were supported by inhibition of GlmU acetyltransferase activity with two different inhibitors, suggesting the involvement of this enzyme in the *M. smegmatis* defence mechanisms.

1. Introduction

Living species are continuously subjected to alkylating stress by both endogenous and exogenous species that can covalently modify metabolites and biological macromolecules. Particularly, DNA can be alkylated by reactive species leading to the generation of miscoding bases possibly providing lethal modifications in genetic information [1].

Methylating agents, like methyl methane sulphonate (MMS), consist in a large category of reactive chemical compounds that can attack nucleophilic sites on DNA bases causing covalent modifications [2–4]. DNA modification seriously impairs transcription and replication or disorganizes the cell-cycle checkpoints driving eukaryotic cells to apoptosis. Since these molecules are ubiquitous and hence unavoidable, all living organisms have developed several repair or defence mechanisms to overcome their effects and to protect the DNA molecule. Many bacteria build up inducible response pathways that enhance cellular resistance to defend against unpredictable levels of environmental alkylating agents [5–14].

Alkylation response mechanisms also occur in *Mycobacterium tuberculosis* (MTB), a non sporogenous aerobic pathogenic bacterium, responsible for tuberculosis disease (TB), still one of the most important cause of death due to a unique pathogen. A distinguishing feature of MTB is the presence of a complex cell wall

* Corresponding author. Department of Chemical Sciences, University of Naples "Federico II", Via Cintia 6, 80126, Naples, Italy.
E-mail address: anduilio@unina.it (A. Duilio).
[1] Equal contribution/co-first authors.

https://doi.org/10.1016/j.resmic.2019.03.002
0923-2508/

much thicker than in other bacteria, characterized by a high concentration of extremely long chain lipids. This cellular architecture, which confers resistance to environmental factors and antibiotic substances, is important in the pathogenicity of tuberculosis infection because it can affect immune response and granuloma formation [15,16]. Current therapeutic treatments of TB disease require the use of multiple anti-mycobacterial drugs such as rifampicin and isoniazid [17].

Recently we demonstrated that treatment of *Escherichia coli* with small amounts of MMS caused a strong decrease in biofilm formation due to the reduced expression of the enzyme NanA [18]. A global investigation of *Mycobacterium smegmatis* response to alkylating agents was then pursued by differential proteomics to evaluate the protein expression profiles under alkylating stress conditions and to identify the most affected cellular pathways.

Surprisingly, contrary to *E. coli*, when we incubated *M. smegmatis* with a sublethal amount of MMS a strong increase in biofilm formation was detected. Quantitative analysis of proteomic profiles demonstrated that most of the *M. smegmatis* proteins upregulated following MMS treatment are involved in biofilm formation and/or cell wall biosynthesis. Tailored experiments confirmed that under stress conditions *M. smegmatis* elicits physical defence mechanisms by increasing biofilm formation. Among the upregulated proteins, we focused our attention on the bifunctional enzyme GlmU whose expression was largely increased under biofilm inducing conditions and that was reported to be involved in biofilm production in *E. coli*, *Staphylococcus epidermidis* and *Staphylococcus aureus* [19–21]. Experiments with both conditional deletion and overexpressing *glmU* mutants suggested that down regulation of GlmU decreased *M. smegmatis* capabilities to produce biofilm whereas overexpression of the enzyme increased biofilm formation. These data were further supported by inhibition of GlmU acetyltransferase activity with two different inhibitors resulting in a clear decrease of biofilm formation, thus confirming the role of GlmU in the process of biofilm production in *M. smegmatis*.

2. Materials and methods

2.1. M. smegmatis *and MTB culture*

M. smegmatis wild type cells were grown 3 days in 7H9 medium, supplemented with 10% ADC, containing 0.05% tween 80 at 37 °C. Saturated *M. smegmatis* cultures were diluted to 0.05 OD in fresh medium; cells were divided in aliquots and treated with MMS in a 0.01–0.07% w/v range for 24 h. Bacterial cultures were serially diluted and incubated on 7H11 plate supplemented with 10% OADC at 37 °C. Cell viability was determined by enumerating CFUs after four days incubation. Growth profiles were obtained by monitoring cells for 30 h with and without MMS treatment.

Saturated MTB cultures were diluted to 0.05 OD in 7H9 liquid medium supplemented with 10% ADC [22] and grown for 15 days. A_{600} was measured every 48 h for 8 days. At day 8; 0.03% or 0.015% MMS or specific drug were added., Cell viability was evaluated at day 11, 13 and 15 by enumerating CFUs. Experiments were performed in triplicate. Cells detection was performed by Ziehl-Neelsen acid-fast staining [22]. MIC measurements were performed with the help of Resazurin Microtiter Assay (REMA) as described earlier [23]. Briefly, wells of a 96 well microtitre plate were filled with 50 μl of 7H9 media and serial dilutions of antibiotic were added. The last column was left untreated and used as a control. *M. smegmatis* strains were grown in replicates in 7H9 medium to an A_{600} ~0.6; diluted 1000 times, and 50 μl of the diluted culture was added to each well. After 40 h of incubation, 30 μl of resazurin dye was added to all the well and incubated for 6 h under shaking and imaged. MICs were determined as the values of the first well showing no growth as indicated by resazurin dye staining.

2.2. Differential Gel Electrophoresis (DIGE)

Protein extracts from MMS treated *M. smegmatis* (MMS_SMEG) and untreated *M. smegmatis* (control_SMEG) cells were analyzed by DIGE procedure [24,25]. Four independent gels were performed in order to obtain statistically significant data. The protein extracts were resuspended in buffer containing 0.03 M Tris-HCl pH 7.5, 7 M urea, 2 M thiourea and 4% chaps. Equal amounts of protein lysates from MMS treated and control cells were labeled *in vitro* using Cy3 and Cy5 cyanine minimal dyes respectively (GE Healthcare, Piscataway, NJ). A third cyanine dye (Cy2) was used to label a mixture of the two samples used as internal standard [26,27]. The first dimension separation was performed using 18 cm IPG strips, 3-10NL pH range. Labeled proteins were loaded on the strips and electrofocused overnight (75 kV/h) at 20 °C. The focused proteins were reduced in equilibration buffer containing 0.5% dithiothreitol for 15 min and alkylated with 4.5% iodoacetamide for a further 15 min. SDS-PAGE was performed using 10% polyacrylamide gels (20 × 24 cm) onto Ettan Dalt Twelve system (GE Healthcare, Piscataway, NJ) overnight at 2 W for each gel. The fluorescent images were acquired at excitation/emission values of 488/520, 532/580, 633/670 nm, at 100 μm resolution, using a Typhoon 9400 Variable Mode Imager (GE Healthcare, Piscataway, NJ). Images were processed by DeCyder v5.2 software (GE Healthcare) in Batch Processing mode performing the detection and quantification of protein spots in Differential In-Gel (DIA) module and spot matching in Biological Variation Analysis (BVA) module, as previously described [28]. According to DIGE procedure, the fluorescence intensity was associated to each selected spot. In order to reduce inter-gel variation, the spot biological fold change was expressed as a mean value of the four biological samples. Finally, spot intensities were compared between MMS treated and control gels and the spot variation was evaluated by statistic *t-test*. We included protein spots with fold change>1.20 and $p < 0.05$ in the image analysis. The accepted spot matching was checked by manual inspection.

2.3. Proteomic analysis

Protein extract (500 μg) from four biological replicates of MMS_SMEG and from four biological replicates of control_SMEG were used to perform a preparative gel. Gel was stained using fluorescent dye Sypro Ruby (Molecular Probes Inc., Eugene, OR) [29]. Selected spots were excised, hydrolyzed and processed by LC-MS/MS as described earlier [30]. The MS/MS spectra raw data were processed by in-house Mascot software (version 2.4) [31]. The Mascot research parameters were the following: *M. smegmatis* protein database; trypsin as proteolytic enzyme; up to 1 missed cleavage; 200 ppm mass tolerance for precursor ions; 0.8 Da mass tolerance for fragment ions, S-carbamidomethylcysteine as fixed modification, pyro-Glu formation (from N-term Gln) and Met oxidation as variable modifications. Peptides, displaying an individual MASCOT score > 38 were considered significant for identification [32,33].

2.4. Clustering analysis

The 'STRING: functional protein association networks' 7.0 software (http://string-db.org/) was used to analyse identified protein dataset. The STRING database allowed us to define the physical (direct) and functional (indirect) protein interactions. Identified proteins were assembled into significant canonical pathways or

networks according to their associated score, defined as the negative logarithm of the p-value [34].

2.5. Generation of MsΔglmU gene replacement mutant

M. tuberculosis glmU gene was digested with NdeI-HindIII from pQE2-$glmU_{Mtb}$ construct and sub-cloned into the corresponding sites on pST-KirT vector [35,36] *M. smegmatis* mc^2155 (*Ms*) strain was electroporated with pST-$glmU_{tet\text{-}off}$ construct to generate a merodiploid strain *Ms*::*glmU*. Approximately 1 kb upstream and downstream flanking sequences of $glmU_{Msm}$ were amplified followed by the generation of AES, which was subsequently cloned into phAE159 to generate temperature sensitive phagemid [35,37]. *MsΔglmU* conditional mutant was generated from *Ms*::*glmU* using specialized transduction [37]. Genomic DNA was isolated from the wild type (*Ms*) and the potential mutant (*MsΔglmU*) and the recombination at the native locus was confirmed by PCR.

2.6. Generation of MspNitglmU overexpressing mutant

M. tuberculosis glmU from pQE2-$glmU_{Mtb}$ construct was released with NdeI-HindIII and subcloned into the corresponding sites to modified pNit1 construct [38] containing apramycin resistance gene. *M. smegmatis* was electroporated with pNit-Apra-glmU construct to generate *Ms*::*pNit-glmU* strain. In the presence of isovaleronitrile (IVN) the strain overexpresses GlmU.

2.7. Growth and scanning electron microscopy (SEM)analysis

For monitoring growth on plates, cultures of *M. smegmatis* (*Ms*), *M. smegmatis* merodiploid (*Ms*::*glmU*) and *MsΔglmU* (*ΔglmU*) were grown in the absence of ATc till A_{600} of 0.8 and streaked on 7H11 agar plates with or without ATc. To evaluate the growth pattern, A_{600} ~0.8 cultures of *Ms* and *ΔglmU* grown in the absence of ATc were seeded at A_{600} ~0.02 and growth was monitored every 3 h for 30 h. For SEM analysis, cultures were grown for 9 or 12 h in the presence or absence of ATc and the samples were processed for SEM as described earlier [37].

2.8. Static biofilm assay

M. smegmatis (WT) and *MsΔglmU* (*ΔglmU*) conditional mutant strains were grown overnight in the absence of ATc. The cultures were seeded in triplicate for each experiment (Crystal Violet assay and CFU analysis) at A_{600}~ 0.05 in Sauton's medium (200 μl) in a sterile 96 well plates. ATc was added to WT samples at 24 h and in control *ΔglmU* sample ATc was not added. In other *ΔglmU* samples ATc was added at different time points after starting the culture (24, 48, 72 and 96 h). All the samples were analyzed for biofilm formation and viability after 120 h (5 days) by both crystal violet and CFU analysis respectively.

M. smegmatis cultures were freshly streaked on 7H11 agar plates and grown for 24 h at 37 °C. 2–3 colonies were inoculated in 7H9 medium + ADC for 16 h at 37 °C. Saturated *M. smegmatis* cultures were seeded in triplicate at A600 of 0.05 OD in Sauton's medium (200 μl) in a sterile 96 well plates. Cultures were incubated at 30 °C for 4 days and then treated with 0.03% or 0.05% (w/v) MMS in the absence and in the presence of either 20 μM iodoacetamide (IAA) or 20 mM N-acetylglucosamine-1-phosphate (GlcNAc1P) for 24 h. All the samples were analyzed for biofilm formation and the IAA treated sample was also monitored for cell growth.

Crystal violet assays were performed as follows: bacterial cells were removed and the biofilm containing wells were washed twice with sterile water. Wells were then dried at RT and 200 μl 0.1% crystal violet was added and incubated at RT for 20–30 min The dye was removed, wells were washed with sterile water and 200 μl of destaining solution (80% ethanol-20% acetic acid) was added at room temperature and incubated for 20–30 min. The absorbance was measured at 590 nm.

3. Results

3.1. MMS effect on M. smegmatis cells

Preliminary experiments were carried out on *M. smegmatis* to evaluate the lowest amount of MMS clearly affecting cells growth. *M. smegmatis* cells were grown with and without different concentrations of MMS (0.01–0.07% w/v) and the bacterial culture viability was determined by measuring CFUs. Fig. 1A shows a decrease in cell viability with increasing doses of MMS in comparison with untreated cells. A concentration of 0.03% MMS led to a decrease of about 50% cell viability. The growth profiles of *M. smegmatis* with and without 0.03% MMS were then evaluated (Fig. 1B) confirming a slight effect of the alkylating agent on bacterial growth, and this concentration was used for further studies.

3.2. MMS on M. tuberculosis clinical strains

The effect of methylation stress on MTB was investigated to explore whether limited doses of alkylating agents might also affect MTB cell viability using MMS as methyl donor. Alkylation experiments were performed on two reference (H37Rv and H37Ra) and 4 different tubercular strains of *M. tuberculosis* three of which had developed drug resistance (strain 100/12 resistant to isoniazid, strain 223/12 resistant to streptomycin and strain 1726/11 resistant to both isoniazid and rifampicin) and on 4 different species of mycobacterium (*Mycobacterium gordonae, Mycobacterium szulgai, Mycobacterium xenopi* and *Mycobacterium chelone*). The Minimum Inhibitory Concentrations (MIC) of MMS for both reference strains were calculated by REMA assay [23] and were 0.1% and 0.05% for H37Rv and H37Ra respectively. Alkylation experiments were carried out in triplicate and cell viability was evaluated by numbering CFUs after 4 days incubation. When the bacteria cultures were exposed to MMS treatment (0.03% or 0.015% w/v), seven out of eight mycobacteria samples appeared sensitive to MMS showing decreased cell viability in these conditions. Fig. 1C shows the number of viable colonies of strain 100/12 resistant to isoniazid (0,2 μg/mL), following treatment with MMS in comparison with untreated cells or cells treated with isoniazid. The viability of strain 100/12 was affected by both MMS concentrations whereas the isoniazid treatment was clearly ineffective.

These results were confirmed by microscopy of mycobacterial cells. Fig. 2 shows the optical microscopy images of strain 100/12 in all conditions tested. In the presence of both MMS concentrations (Panels C and D), a remarkable disappearance of the typical mycobacterial cells clusters was clearly detected with respect to control samples (Panel A) while isoniazid treated cells did not show significant differences compared with the control cells (Panels A and B).

3.3. Comparative proteomic analysis

Since alkylating stress affected mycobacterial viability, a comprehensive investigation of *M. smegmatis* response to alkylating stress at the molecular level was then pursued by comparative proteomics. Four biological replicates of *M. smegmatis* were treated with 0.03% MMS. Untreated cells were used as negative control. Following 3 h incubation, cellular extracts from MMS treated and untreated *M. smegmatis* cell cultures were labelled with fluorescence dyes and fractionated by 2D electrophoresis according to the DIGE technology [39], using a 3–10 pH gradient (Fig. 3A).

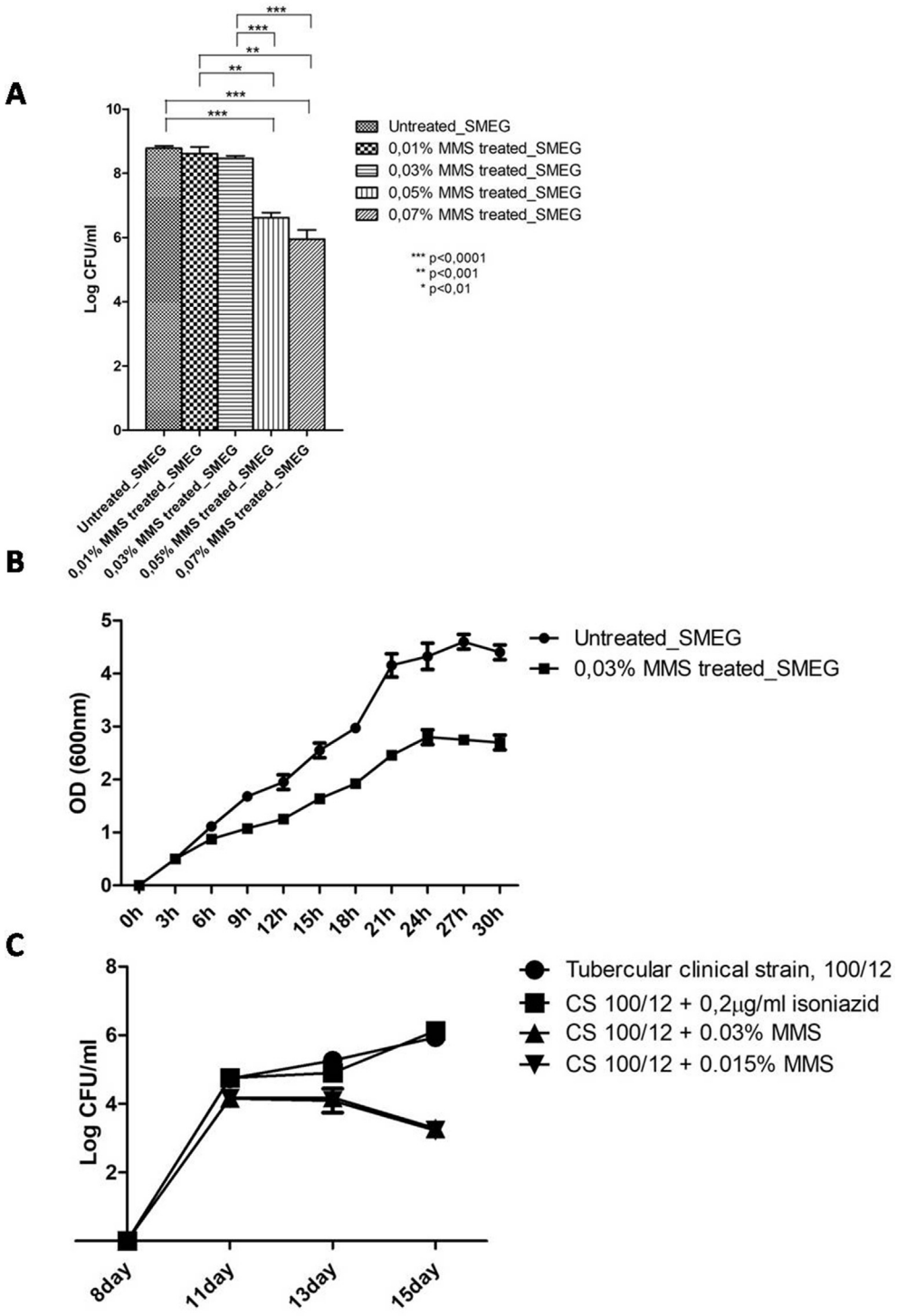

Fig. 1. **A**: *M. smegmatis* wild type cells were treated with 0.01% (w/v), 0.03% (w/v), 0.05% (w/v), 0.07% (w/v) MMS and cell viability was evaluated by enumerating CFUs after four days incubation in comparison with untreated cells. Experiments were run in triplicate and the error bars on the graphs stand for the standard deviation from the mean of the 3 experiments. One way ANOVA statistical test using Graph pad prism software was performed. **B**: Growth profiles of *M. smegmatis* cells in the absence (circle) and in the presence (square) of 0.03% MMS. Experiments were run in duplicate and the standard deviation is reported as error bars. **C**: Number of viable colonies observed in the *M. tuberculosis* clinical strain 100/12 resistant to isoniazid in the presence of 0,2 µg/mL isoniazid (square), 0.03% MMS (up triangle) and 0.015% MMS (down triangle). Circles refer to control cells. Cell viability was evaluated by enumerating CFUs on samples withdrawn from bacterial cultures at 11, 13 and 15 days after four days incubation. The error bars on the graph are represented as the standard deviation from the mean of 3 experiments.

Comparative and quantitative analyses were performed and the up- or downregulated proteins with a statistically significant fold-change were defined. The MMS treated sample was then run on a preparative gel in the same conditions and stained with Sypro Ruby (Fig. 3B). Stained spots matching the corresponding DIGE analytical gels were selected for identification by mass spectrometry and the mass spectral data were processed by an in-house version of the Mascot software. A total of 71 differentially expressed proteins were identified and the results are summarized in Supplemental Table 1. For each protein, the fold change, spot number, protein

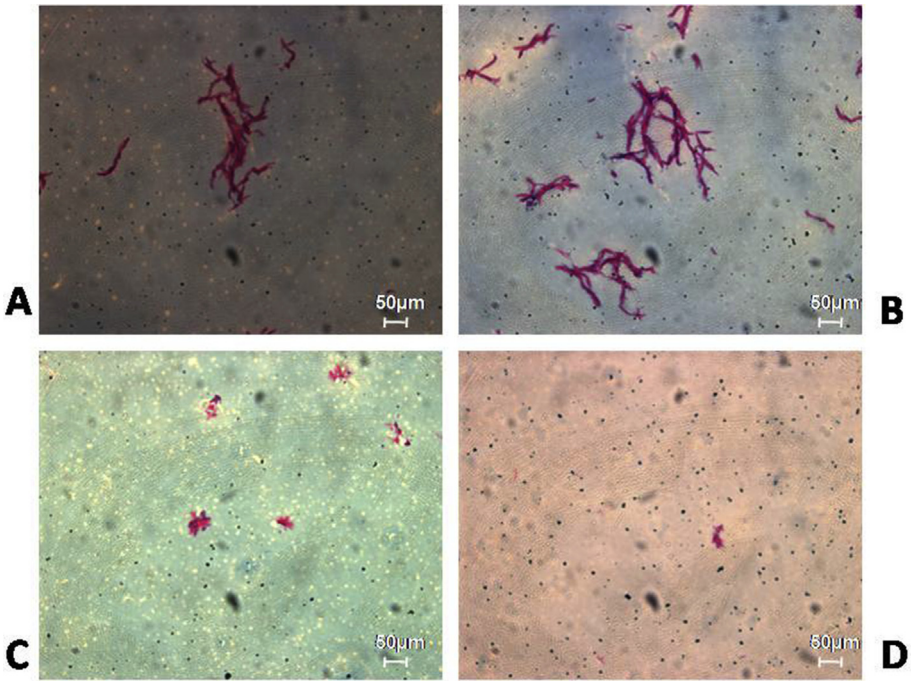

Fig. 2. Optical microscopy images of the *M. tuberculosis* clinical strain 100/12 resistant to isoniazid observed following incubation with isoniazid (B) or in the presence of 0.015% MMS (C) or 0.03% MMS (D). Control cells images are reported in Panel A for comparison. Scale bars 50 μm, enlargement 100-fold.

description, gene official symbol, Swiss-Prot. Code, Mascot Score and number of identified peptides are reported.

3.4. Biological networks and functional annotation analysis

The STRING functional protein interaction networks (http://string-db.org/) and DAVID Bioinformatics Resources (https://david.ncifcrf.gov/) were used to evaluate the network distributions of the 71 identified differentially expressed proteins.

Among the up-regulated proteins, the STRING analysis revealed a large network comprising most of the identified proteins (43 out of 71; number of edges 74, clustering coefficient 2.71 and enrichment p-value 4.38e-07). Data are reported in Supplementary Fig. 1. Stronger associations are represented by thicker lines. Within this network, a subcluster including 6 proteins, Chaperone protein DnaK (DnaK), DNA gyrase subunit B (GyrB), Peptidyl-prolylcis-trans isomerase (PpiA), 60 kDa chaperonin 1 (GroEL1), Alanine-tRNA ligase (AlaS) and Inosine-5′-monophosphate dehydrogenase (GuaB), was detected. All these proteins were reported to be involved in biofilm formation to varying degrees [40,41].

When the DAVID database [42] was used to examine the identified upregulated proteins, 11 proteins were found involved in metabolic pathways gathering within the Glycan Biosynthesis and Metabolism area. Among these, the enzyme GlmU was reported to be involved in biofilm production of several pathogenic and nonpathogenic bacteria [19,21,43], whereas LeuD and VanX are involved at different levels in cell wall biosynthesis to produce peptidoglycan chain precursors [22,44] These results suggest that MMS treatment of *M. smegmatis* gave rise to an increase in the expression of proteins contributing to defence mechanisms involving cell wall architecture and biofilm formation.

3.5. Effect of methylation stress on biofilm formation in M. smegmatis

The overexpression of proteins involved in biofilm formation as a result of methylation stress prompted us to perform specific assays to evaluate the amount of biofilm formed by *M. smegmatis* with and without MMS.

Static growth conditions were preliminarily optimized in order to accurately measure biofilm formation. *M. smegmatis* was inoculated in wells and incubated at 30 °C for 4 days in 7H9 medium. Cells were then treated with either 0.03% or 0.05% MMS and quantification of attached cells was determined after 24 h by crystal violet staining and subsequent measurement of absorbance at 590 nm. Experiments were performed in triplicate and the averaged data are reported in Fig. 4. Methylation stress induced by MMS treatment increased biofilm production compared to untreated cells in a dose-dependent manner. Cell viability was evaluated by CFUs measurements at both MMS concentrations according to Fig. 1A. This finding was in agreement with proteomic results suggesting that *M. smegmatis* response to damaging events led to increasing biofilm production mechanisms. It should be underlined that in the same conditions, MMS treatment strongly decreased biofilm formation in *E. coli* [18].

3.6. GlmU is essential for biofilm formation in M. smegmatis

Differential proteomics results suggested that MMS treatment of *M. smegmatis* increased the expression of proteins involved in biofilm formation. Among these, the expression of GlmU was upregulated by almost 50 fold under biofilm inducing conditions. Moreover, GlmU was reported to play a role in biofilm formation in *E. coli*, *S. epidermidis* and *S. aureus* being involved in the synthesis of an essential precursor required for biofilm production [19–21,43]. On this ground, we pursued a detailed investigation to assess the putative role of GlmU in biofilm formation in *M. smegmatis*, if any.

Biofilm production in *M. smegmatis* was evaluated in the absence of GlmU. *glmU* is an essential gene and hence a mutant can only be generated in the presence of an inducible copy. We utilized previously developed integrative construct pST-KirT-glmU [35,36] herein the expression of *glmU* is under the regulation of tetracycline inducible promoter [45]. The promoter is functional in the absence of anhydotetracylin (ATc) and addition of ATc shuts off the

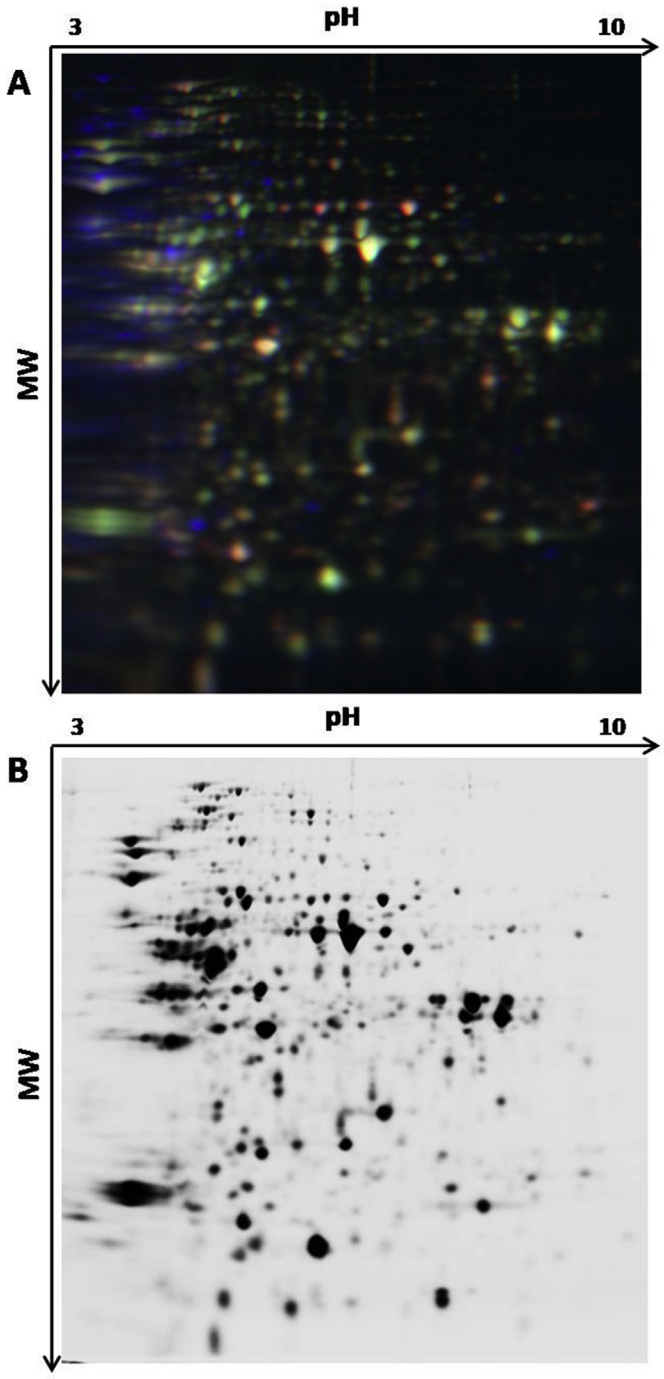

Fig. 3. Differential in Gel Electrophoresis (DIGE) of protein extracts from MMS treated and untreated *M. smegmatis* cells. **A**: Superimposed images of the individual fluorescent scans of analytical gel. Equal amounts of protein lysates from four biological replicates were labeled *in vitro* using Cy3 (red fluorescence, MMS treated) and Cy5 (green fluorescence, MMS untreated) dyes. A third cyanine dye (yellow fluorescence, Cy2) was used to label a mixture of the two samples used as internal standard. **B**: Semi-preparative 2D-Gel Electrophoresis of protein extracts from *M. smegmatis* cells treated with MMS. Protein extracts from four biological replicates of MMS treated and four biological replicates of control MMS untreated *M. smegmatis* cells were run a preparative gel stained with Sypro Ruby. Individual spots were used for protein identification.

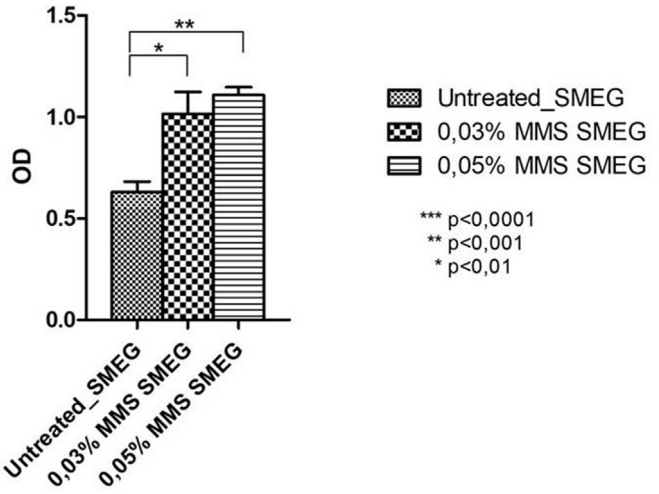

Fig. 4. Biofilm formation in *M. smegmatis* under different conditions. *M. smegmatis* cells were incubated in triplicate at 30 °C for 4 days and then treated with either 0.03% or 0.05% (w/v) MMS for 24 h. Biofilm formation was evaluated by crystal violet assay in comparison with control cells. The error bars on the graph stand for the standard deviation from the mean of 3 experiments. One way ANOVA statistical test using Graph pad prism software was performed.

expression of the enzyme. In order to generate *glmU* mutant in *M. smegmatis*, pST-KirT-glmU was electroporated to generate the merodiploid (Fig. 5A). The *glmU* at native locus was replaced with *hyg*^{r} marker and the recombination at the native locus was confirmed by PCR (Fig. 5B). Two independent recombinants were streaked along with *M. smegmatis* (*Ms*) and merodiploid (*Ms*::*glmU*) strains in the presence or absence of ATc (Fig. 5C). It is clear from the data that the recombinants failed to grow in the presence of ATc. Western blot analysis of wild type (*Ms*) and mutant (*Ms*::*glmU*) in the absence and presence of ATc showed that the growth defect observed was indeed due to the depletion of GlmU (Fig. 5D). Growth pattern analysis performed in the absence or presence of ATc was in agreement with the above data (Fig. 5E). SEM analysis, performed to evaluate the impact of GlmU depletion on morphology, showed presence of significant number of fused cells with wrinkled surface (Fig. 5F).

Next we set out to evaluate the role of GlmU in biofilm production using the *MsΔglmU* mutant. *M. smegmatis* and *MsΔglmU* strains were grown at 30 °C in triplicate in multiwell plate. Both biofilm formation and cell viability of the *MsΔglmU* mutant used as control were measured just before the addition of ATc and the corresponding values are shown in Fig. 6A and B (*MsΔglmU-ATc*, second bar in the figures). The expression of GlmU was then inhibited by adding 200 ng of ATc at different time points, 24, 48, 72 and 96 h, in different wells of *MsΔglmU*. ATc was shown to have no effect on wild type *M. smegmatis* culture (first bar in Fig. 6A and B).

As shown in Fig. 6A, when *MsΔglmU* cultures were treated with ATc after 24 or 48 h of growth, a decrease of about 82% or 68% respectively in biofilm formation was observed (Fig. 6A, third and fourth bars) suggesting that depletion of GlmU at the early phase of growth might impair biofilm production underlining a possible involvement of GlmU in this process. No significant differences in biofilm formation were detected when GlmU depletion was induced at late stage of cell growth (Fig. 6A, fifth and sixth bars), indicating that depletion of GlmU was ineffective when maximum biofilm production had already occurred.

Then, we performed a similar experiment and determined cell viability in *M. smegmatis* and the *MsΔglmU* mutant either in the absence (*MsΔglmU-ATc*) or in the presence (*MsΔglmU* + *ATc*) of ATc. Fig. 6B shows that following 24 h ATc treatment a large decrease in cell viability of the *MsΔglmU* mutant was observed whereas no significant differences in cell density were observed between *MsΔglmU-ATc* and *MsΔglmU* + *ATc* cultures when ATc was added at

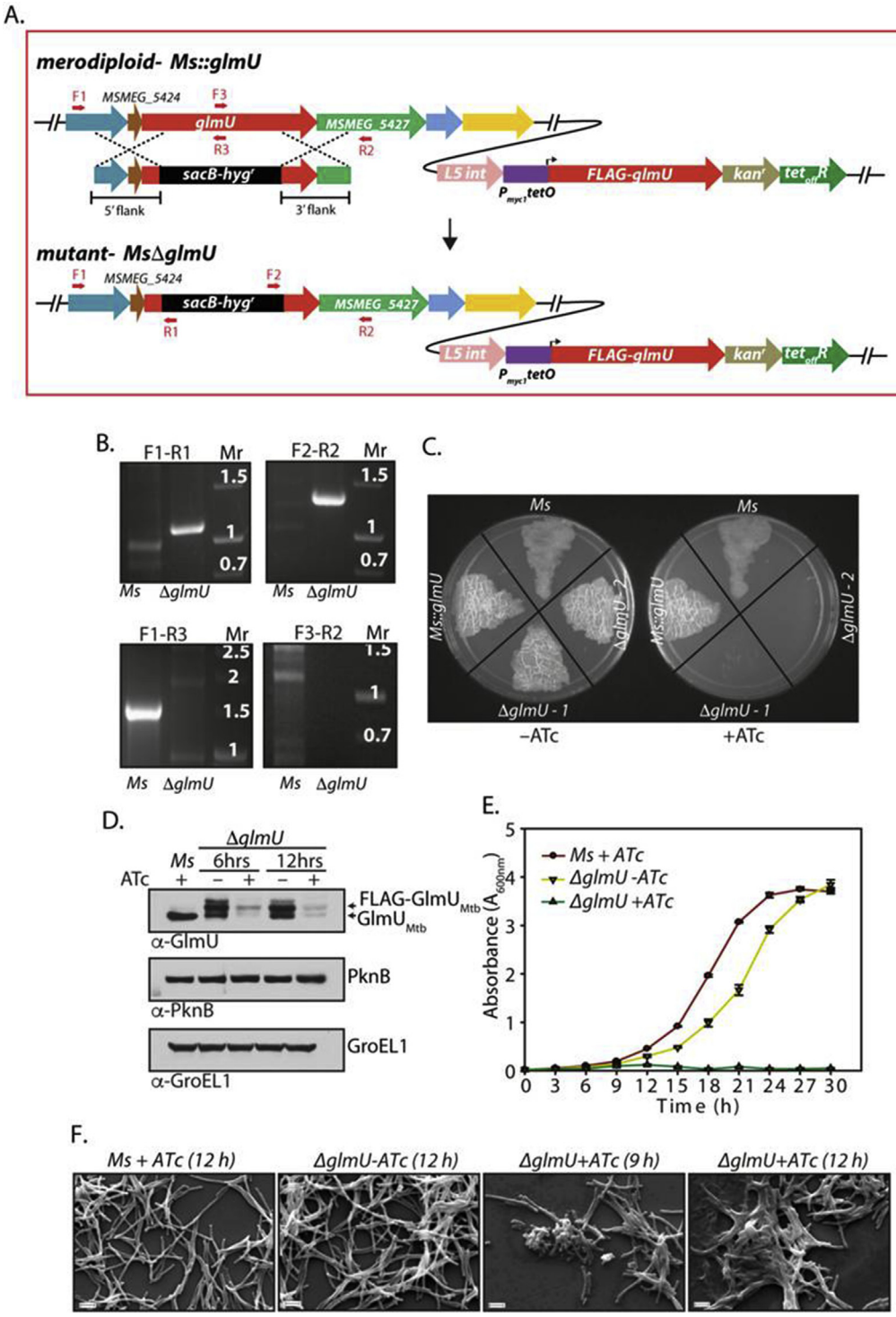

Fig. 5. A Schematic diagram representing the genomic location of *glmU* (MSMEG_5426) and homologous recombination between flanking sequence in the phagemid and the genomic locus. **B** Agarose gel showing the PCR amplification of the *Ms* & putative *ΔglmU* mutant using specific primers. Primers F1 and R2 are beyond the flanks, R1 and F2 belongs to resolvase sites in sacB/hygR cassette and F3 and R3 binds to the native *glmU*. Amplification with F1-R1 or F2-R2 primers results in 1.08 kb or 1.29 kb size products with *ΔglmU* strain but none with the *Ms*. Whereas PCRs with F1-R3 or F3-R2 primers amplifies 1.6 kb or 1.26 kb band with the *Ms* and none with the *ΔglmU* mutant. **C**. *Ms*, *Ms*::*glmU* and *ΔglmU* cultures grown to an A600 of 0.8 OD and streaked on 7H11 agar plates with or without ATc. **D**. Western blots showing endogenous GlmU and FLAG-GlmU at 6 h & 12 h post ATc addition. For loading control PknB and GroEL1 were probed. **E**. Growth curve analysis of *Ms* and *ΔglmU* in presence or absence of ATc up to 30 h. **F**. SEM images of *Ms* and *ΔglmU* at 9 h and 12 h after the addition of ATc. Scale bars 2 μm.

72 and 96 h (Fig. 6B, fifth and sixth bars). These data raised the question whether the reduced biofilm formation had to be ascribed to a decrease in the replication rate of *MsΔglmU* when the expression of GlmU was stopped as this enzyme is essential for growth, or to a specific role exerted by GlmU itself.

In an attempt to solve the question, we tested whether the overexpression of GlmU had an effect on biofilm formation. We used a newly developed integrative construct where the expression of *glmU* is under the control of isovaleronitrile (IVN) inducible promoter (*Ms.pNit-glmU*) [38]. *M. Smegmatis* and *Ms.pNit-glmU*

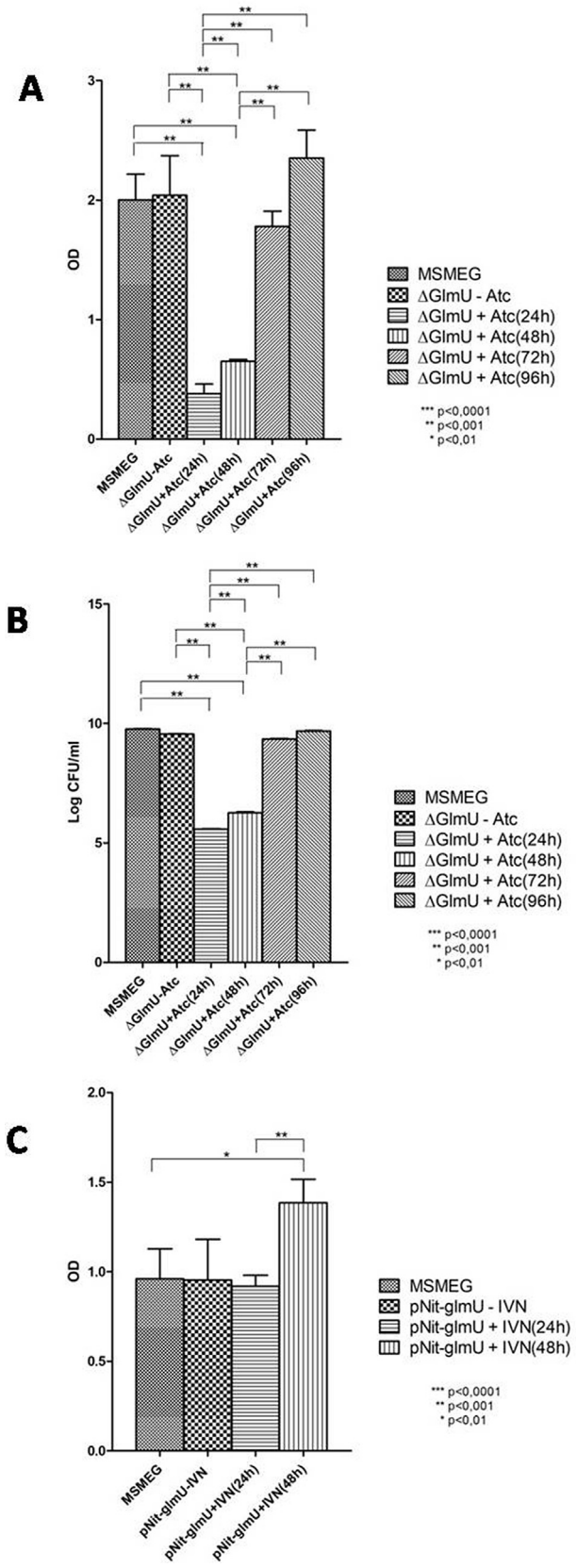

Fig. 6. A: *M. smegmatis* and *Ms⊿glmU* conditional deletion mutant strains were grown in triplicate in multiwall plate. Formation of biofilm was measured by crystal violet assay after five days of growth. Second bar in the figure shows biofilm formation of the *Ms⊿glmU* mutant used as control just before the addition of ATc. The expression of GlmU was then inhibited by adding 200 ng of ATc at different time points, 24, 48, 72 and 96 h, in different wells of *Ms⊿glmU*. The error bars on the graphs stand for the standard deviation from the mean of 3 experiments. One way ANOVA statistical test using Graph pad prism software was performed, $p < 0.0001$. **B:** The experiment was performed as described above, colonies were counted and $\log_{10}$ CFU/ml values were calculated and plotted using graph pad prism software. Second bar in the figure shows the cell viability of the *Ms⊿glmU* mutant used as control just before the addition of ATc. The error bars on the graphs stand for the standard deviation from the mean of 3 experiments. One way ANOVA statistical test using Graph pad prism software was performed. **C:** *M. Smegmatis* and *Ms.pNit-glmU* overexpressing mutant strains were grown in triplicate in multiwall plate. Biofilm formation of the *Ms.pNit-glmU* mutant used as control was measured just before the addition of IVN (*Ms.pNit-glmU-IVN*, second bar in the figure). After 48 h, 5 μM IVN was added in different wells of *Ms-pNit-glmU* to induce the overexpression of GlmU. Formation of biofilm was measured by crystal violet assay after five days of growth. The error bars on the graphs stand for the standard deviation from the mean of 3 experiments. One way ANOVA statistical test using Graph pad prism software was performed.

strains were grown at 30 °C in triplicate in multiwall plate. Biofilm formation of the *Ms.pNit-glmU* mutant used as control was measured just before the addition of IVN and the corresponding values are shown in Fig. 6C (*Ms.pNit-glmU-IVN*, second bar in the figure).

The expression of GlmU was then induced at 48 h in the *Ms-pNit-glmU* mutant by treatment with 5 μM IVN. At five days of growth, crystal violet assay was performed to measure the formation of biofilm and the cell density was determined by measuring the absorbance at 590 nm. As shown in Fig. 6C, following IVN stimulation at 48 h *Ms.pNit-glmU* showed a 45% enhancement of biofilm formation (*Ms.pNit-glmU + IVN*, third bar in the figure), indicating that increasing amount of GlmU impacted biofilm production and suggesting a role of the enzyme in this process.

3.7. GlmU inhibition and biofilm formation in M. smegmatis

To further define whether or not GlmU had a role in biofilm formation in *M. smegmatis*, we measured biofilm levels following inhibition of the acetyltransferase domain of GlmU. Several authors reported that inhibition of GlmU by thiol-specific reagents [19,20,46,47] or its reaction product N-acetylglucosamine-1-phosphate [21,48–51] resulted in decrease of biofilm production in various microorganisms with only a slight effect on bacterial growth.

The amount of biofilm produced by *M. smegmatis* under methylation stress conditions was measured in the presence of different concentrations of iodoacetamide (IAA), a GlmU acetyltransferase domain inhibitor [19,46]. Fig. 7A shows that inhibition of GlmU by 20 μM IAA decreased biofilm levels induced by MMS treatment. The growth profiles of *M. smegmatis* in the presence of 20 μM IAA was also evaluated indicating only a slight effect of the chemical agent on bacterial growth that in these conditions was still able to grow (Fig. 7B).

A further GlmU inhibition experiments was then performed in the presence of N-Acetylglucosamine-1-phosphate (GlcNAc-1P), a competitive inhibitor of GlmU [48–50]. Biofilm formation was then measured following MMS treatment of *M. smegmatis* cells in the presence of 20 mM GlcNAc-1P. Inhibition of GlmU enzymatic activity resulted in a clear decrease of biofilm formation as shown in Fig. 7C.

These data supported the results obtained with GlmU mutants, confirming the involvement of this enzyme in the defence mechanisms elicited by *M. smegmatis* upon alkylation stress.

4. Discussion

Tuberculosis is caused by the mycobacterium *M. tuberculosis*, a pathogen able to survive in the hostile conditions through sophisticated defence mechanisms. In an attempt to clarify some aspects of the *M. tuberculosis* defence mechanisms, we have investigated the

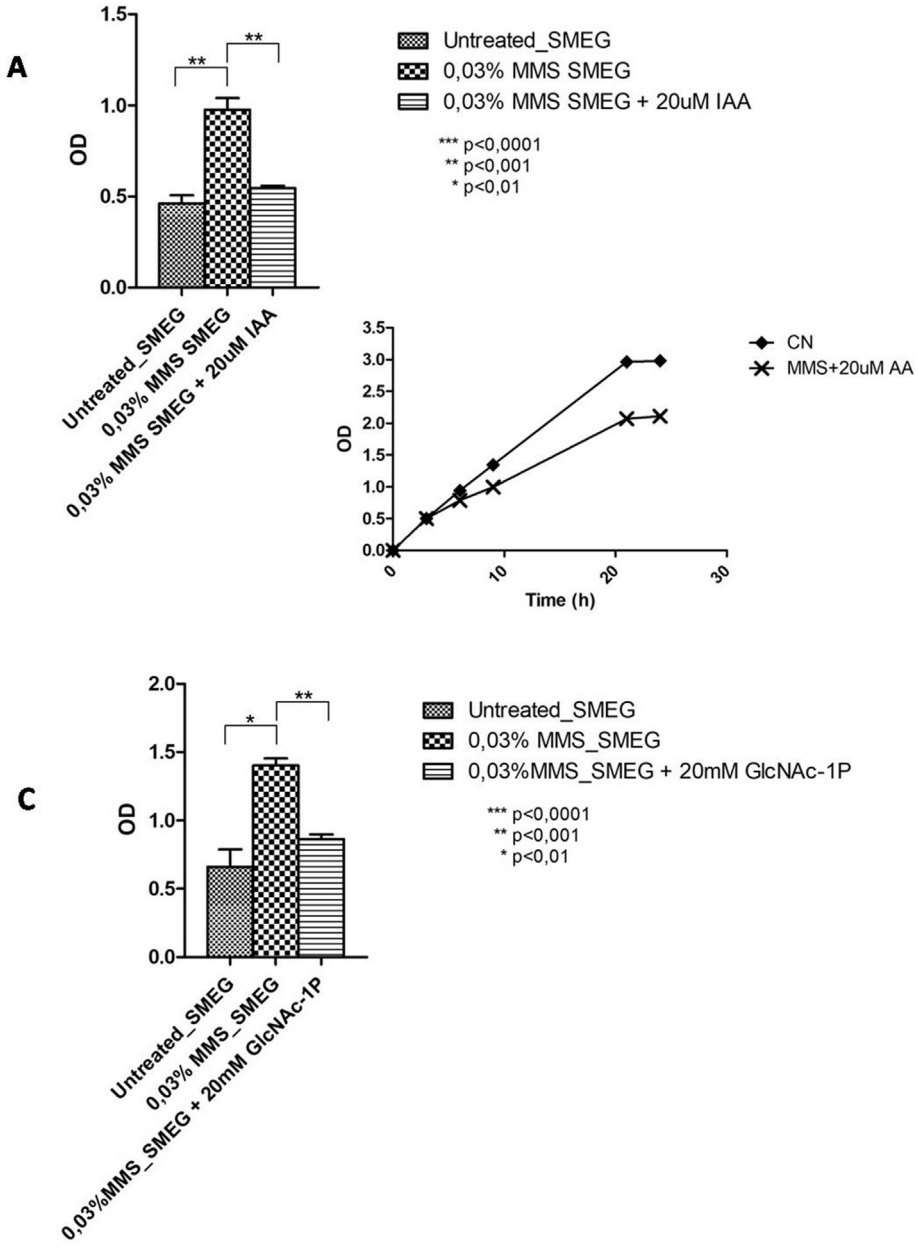

Fig. 7. Biofilm formation in *M. smegmatis* in the presence of acetyltransferase domain inhibitors. *M. smegmatis* cells were incubated in triplicate at 30 °C for 4 days in multiwall plate and then treated with 0.03% MMS for 24 h to induce biofilm formation. **A**: Biofilm production following treatment of *M. smegmatis* with 20 μM iodoacetamide (IAA) for 24 h. Biofilm formation was evaluated by crystal violet assay in comparison with control cells. **B**: Growth profiles of *M. smegmatis* cells in the presence of 0.03% MMS (square), or 0.03% MMS and 20 μM IAA (triangle) in comparison with untreated cells (circle). **C**: Biofilm production in *M. smegmatis* in the presence of 20 mM N-acetyl glucosamine-1-phosphate for 24 h. The error bars on the graphs A, B and C stand for the standard deviation from the mean of 3 experiments. One way ANOVA statistical test using Graph pad prism software was performed.

effect of methylation stress caused by sub-lethal concentration of MMS in clinal strains of *M. tuberculosis* and other tubercular species. Most of mycobacteria appeared sensitive to MMS incubation showing a clear decrease in cell viability, including the strains that had developed isoniazid resistant capabilities.

Recently we demonstrated that treatment of *E. coli* with small amounts of MMS caused a strong decrease in biofilm formation [18]. A global investigation of mycobacteria response to alkylating agents at the molecular level was then performed using *M. smegmatis*, a non pathogenic mycobacteria strain. Surprisingly, contrary to *E. coli*, when treated with a sublethal amount of MMS, *M. smegmatis* showed a clear increase in biofilm formation. Comparative proteomics allowed us to establish that MMS treatment induces upregulation of several proteins involved in cell wall biosynthesis and biofilm formation. Among these, molecular chaperones DnaK and GroEL1 have recently been associated to biofilm formation and stress resistance mechanisms. Chemical inhibition of DnaK was reported to reduce biofilm production in *E. coli* [40] and decreased biofilm formation and adhesion properties in *S. aureus* were observed in the presence of a DnaK non-functional mutation [52]. The GroEL1 protein affects the bio-synthesis of mycolates, crucial components of mycobacterial cell wall, specifically during production of biofilm. Moreover, inactivation of the *groEL1* gene prevented the formation of mature biofilms in *M. smegmatis* [41]. We speculated that the increase in biofilm formation induced by alkylation stress might be part of a more general strategy adopted by mycobacterium to defend itself when submitted to different stress conditions. For instance, biofilm

formation and glmS expression are increased in *E. coli* by exposure to PEG, which mimics an osmotic stress [53].

Clustering analysis of proteomics data showed that several up-regulated proteins gathered within the metabolic pathway leading to peptidoglycan biosynthesis. Among these, we focused our attention on the bifunctional enzyme GlmU whose expression was largely increased under conditions inducing biofilm formation. GlmU is involved in the biosynthesis of UDP-N-acetylglucosamine (UDP-GlcNAc) an essential precursor of β-1,6-N-acetyl-D-glucosamine polysaccharide adhesin needed for biofilm production in *E. coli* and *S. epidermidis* [43]. Moreover, GlmU was reported to play a role in biofilm formation in *Pseudomonas aeruginosa, Klebsiella pneumoniae* and *E. foecalis* [19,21,51].

On this ground, we pursued a detailed investigation on the putative role of GlmU in biofilm production in *M. smegmatis*. We developed a GlmU conditional deletion mutant in which the *glmU* promoter was under the control of Atc (*MsΔglmU*) and an over-expressing mutant where the *glmU* gene was under the control of IVN (*Ms.pNit-glmU*). The *MsΔglmU* mutant showed normal biofilm formation under methylation stress conditions in the absence of ATc. However, a decrease in biofilm production was detected when GlmU was depleted at early stage of cell growth by ATc treatment. On the contrary, an increase in biofilm production was detected when the *Ms.pNit-glmU* mutant was stimulated with IVN, suggesting that increasing amount of GlmU positively affected biofilm production.

However, since the GlmU enzyme is essential for bacterial growth, experiments with *M. smegmatis* mutants might be questionable as the increase/reduction in biofilm formation might also be related to increase/decrease rate of replication of *M. smegmatis* and not directly to GlmU activity. Therefore, to further define whether or not GlmU is involved in biofilm production in *M. smegmatis*, we examined the effect enzymatic inhibitors able to interfere with the GlmU acetyltransferase domain on biofilm formation [19,20,46–50]. In the presence of either IAA or GlcNAc-1P, well known inhibitors of the GlmU acetyltransferase activity, biofilm formation was diminished decreasing to a level very similar to control cells, whereas both cell viability and bacterial growth were only slightly affected.

Altogether these data suggested that GlmU might be involved in the *M. smegmatis* biofilm mediated defence mechanisms. GlmU belongs to a metabolic pathway leading to UDP-GlcNAc from fructose-1-phosphate involved in the biosynthesis of peptidoglycan and lipopolysaccharide (Fig. 8). Recently, we demonstrated that impairment of NanA (N-acetylneuraminate lyase) expression and/or inhibition due to synthetic drugs strongly decrease biofilm formation in *E. coli* [18]. Interestingly, NanA belongs to the same pathway connecting sialic acid metabolism and the amino sugars biosynthesis where GlmU is located, as shown in Fig. 8. Moreover, although the *nanA* gene is absent in *M. smegmatis* genome, NanA and GlmU proteins occur within the proteome of many well known pathogenic bacteria such as *S. aureus* (both NanA and GlmU), *K. pneumoniae* (GlmU) and *P. aeruginosa* (GlmU).

Our findings pointed out to sialic acid metabolism as a key pathway in biofilm production in *M. smegmatis*. Sialic acid and its metabolites GlcNAc and GlcNAc-6-P have long been recognised as signalling molecules in biofilm formation, colonization and host invasion [54]. Moreover, several genes involved in sialic acid metabolism were shown to play a central role in the mechanism of biofilm formation by pathogenic bacteria both *in vitro* and *in vivo* [55,56]. We provided evidence that *glmU* is involved in the biosynthesis and assembly of *M. smegmatis* biofilm protective architecture. Since the reaction catalyzed by the acetyltransferase domain of GlmU is unique to bacteria not having any homology with eukaryotic organisms, these observations might open up the way to the development of compounds that can effectively target this enzyme specifically hampering biofilm formation and avoiding the risk of generating drug-resistant strains.

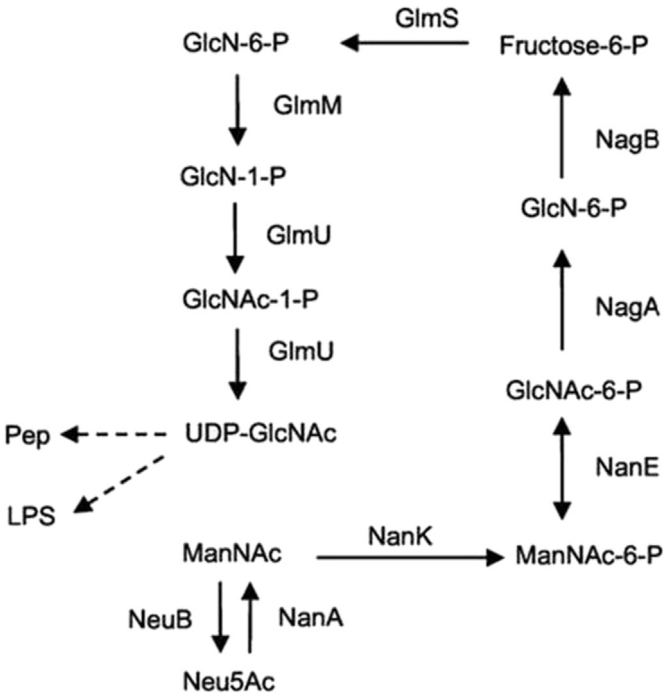

Fig. 8. Pathways of sialic acid and aminosugars metabolism in *E. coli* underlining the relationship between the enzymes NanA and GlmU.

Conflict of interest

The authors declare that they have no conflicts of interest with the contents of this article.

Acknowledgments

We thank Dr. Angelina Cordone for her delicious suggestions. Meetu Agarwal acknowledges the financial support from DBT-RA in Biotechnology and Lifesciences.

Appendix A. Supplementary data

Supplementary data to this article can be found online at https://doi.org/10.1016/j.resmic.2019.03.002.

References

[1] McCarthy TV, Karran P, Lindahl T. Inducible repair of O-alkylated DNA pyrimidines in *Escherichia coli*. EMBO J 1984;3:545–50.
[2] Lobo V, Patil A, Phatak A, Chandra N. Free radicals, antioxidants and functional foods: impact on human health. Phcog Rev 2010;4:118–26.
[3] Teo I, Sedgwick B, Kilpatrick MW, McCarthy TV, Lindahl T. The intracellular signal for induction of resistance to alkylating agents in *E. coli*. Cell 1986;45:315–24.
[4] Taverna P, Sedgwick B. Generation of an endogenous DNA-methylating agent by nitrosation in *Escherichia coli*. J Bacteriol 1996;178:5105–11.
[5] Sedgwick B, Lindahl T. Recent progress on the Ada response for inducible repair of DNA alkylation damage. Oncogene 2002;21:8886–94.
[6] Sedgwick B. Repairing DNA-methylation damage. Nat Rev Mol Cell Biol 2004;5:148–57.
[7] Rippa V, Amoresano A, Esposito C, Landini P, Volkert MR, Duilio A. Specific DNA binding and regulation of its own expression by the AidB protein in Escherichia coli. J Bacteriol 2010;192:6136–42.
[8] Jena NR. DNA damage by reactive species: mechanisms, mutation and repair. J.Biosci. 2012;37:503–17.

[9] Dos Vultos T, Mestre O, Tonjum T, Gicquel B. DNA repair in Mycobacterium tuberculosis revisited. FEMS (Fed Eur Microbiol Soc) Microbiol Rev 2009;33:471–87.
[10] Karran P, Hjelmgren T, Lindahl T. Induction of a DNA glycosylase for N-methylated purines is part of the adaptive response to alkylating agents. Nature 1982;296:770–3.
[11] Volkert MR, Landini P. Transcriptional responses to DNA damage. Curr Opin Microbiol 2001;4:178–85.
[12] Volkert MR, Nguyen DC. Induction of specific Escherichia coli genes by sublethal treatments with alkylating agents. Proc. Natl. Acad. Sci. U. S. A. 1984;81:4110–4.
[13] Landini P, Volkert MR. Regulatory responses of the adaptive response to alkylation damage: a simple regulon with complex regulatory features. J Bacteriol 2000;182:6543–9.
[14] Rippa V, Duilio A, di Pasquale P, Amoresano A, Landini P, Volkert MR. Preferential DNA damage prevention by the E. coli AidB gene: a new mechanism for the protection of specific genes. DNA Repair 2011;10:934–41.
[15] Jankute M, Cox JA, Harrison J, Besra GS. Assembly of the mycobacterial cell wall. Annu Rev Microbiol 2015;69:405–23.
[16] Alderwick LJ, Harrison J, Lloyd GS, Birch HL. The mycobacterial cell wall–peptidoglycan and arabinogalactan. Cold Spring Harb Perspect Med 2015;5:a021113.
[17] Choi R, Jeong BH, Koh WJ, Lee SY. Recommendations for optimizing tuberculosis treatment: therapeutic drug monitoring, pharmacogenetics, and nutritional status considerations. Ann Lab Med 2017;37:97–107.
[18] Di Pasquale P, Caterino M, Di Somma A, Squillace M, Rossi E, Landini P, et al. Exposure of E. coli to DNA-methylating agents impairs biofilm formation and invasion of eukaryotic cells via down regulation of the N-acetylneuraminate lyase NanA. Front Microbiol 2016;7:147.
[19] Burton E, Gawande PV, Yakandawala N, LoVetri K, Zhanel GG, Romeo T, et al. Antibiofilm activity of GlmU enzyme inhibitors against catheter-associated uropathogens. Antimicrob Agents Chemother 2006;50:1835–40.
[20] Suman E, D'souza SJ, Jacob P, Sushruth MR, Kotian MS. Anti-biofilm and anti-adherence activity of Glm-U inhibitors. Indian J Med Sci 2011;65:387–92.
[21] Sharma R, Rao Lambu M, Jamwa U, Rani C2, Chib R, Wazir P, et al. *Escherichia coli* N-Acetylglucosamine-1-Phosphate-Uridyltransferase/Glucosamine-1-Phosphate-Acetyltransferase (GlmU) inhibitory activity of terreic acid isolated from *Aspergillus terreus*. J Biomol Screen 2016;21:342–53.
[22] Chen JW, Scaria J, Chang YF. Phenotypic and transcriptomic response of auxotrophic Mycobacterium avium subsp. paratuberculosis leuD mutant under environmental stress. PLoS One 2012;7:e37884.
[23] Agrawal P, Miryala S, Varshney U. Use of Mycobacterium smegmatis deficient in ADP ribosyltransferase as surrogate for Mycobacterium tuberculosis in drug testing and mutation analysis. PLoS One 2015;13:e0122076.
[24] Imperlini E, Santorelli L, Orrù S, Scolamiero E, Ruoppolo M, Caterino M. Mass spectrometry-based metabolomic and proteomic strategies in organic acidemias. BioMed Res Int 2016;2016:9210408.
[25] Chandler RJ, Caterino M, Sloan JL, Dorko K, Cusmano-Ozog K, Ingenito L, et al. The hepatic proteome of methylmalonic acidemia (MMA): elucidation of altered cellular pathway in humans. Mol Biosyst 2016;12:566–74.
[26] Caterino M, Pastore A, Strozziero MG, Di Giovamberardino G, Imperlini E, Scolamiero E, et al. The proteome of cblC defect: in vivo elucidation of altered cellular pathways in humans. J Inherit Metab Dis 2015;38:969–77.
[27] Capobianco V, Caterino M, Iaffaldano L, Nardelli C, Sirico A, Del Vecchio L, et al. Proteome analysis of human amniotic mesenchymal stem cells (hA-MSCs) reveals impaired antioxidant ability,cytoskeleton and metabolic functionality in maternal obesity. Sci Rep 2016;6:25270.
[28] Barbarani G, Ronchi A, Ruoppolo M, Santorelli L, Steinfelder R, Elangovan S, et al. Unravelling pathways downstream Sox6 induction in K562 erythroid cells by proteomic analysis. Sci Rep 2017;7:14088.
[29] Spaziani S, Imperlini E, Mancini A, Caterino M, Buono P, Orru` S. Insulin-like growth factor 1 receptor signaling induced by supraphysiological doses of IGF-1 in human peripheral blood lymphocytes. Proteomics 2014;14:1623–9.
[30] Caterino M, Aspesi A, Pavesi E, Imperlini E, Pagnozzi D, Ingenito L, et al. Analysis of the interactome of ribosomal protein S19 mutants. Proteomics 2014;14:2286–96.
[31] Imperlini E, Spaziani S, Mancini A, Caterino M, Buono P, Orrù S. Synergistic effect of DHT and IGF-1 hyperstimulation in human peripheral blood lymphocytes. Proteomics 2015;15:1813–8.
[32] Caterino M, Zacchia M, Costanzo M, Bruno G, Arcaniolo D, Trepiccione F, et al. Urine proteomics revealed a significant correlation between urine-fibronectin abundance and estimated-GFR decline in patients with bardet-biedl syndrome. Kidney Blood Press Res 2018;43:89–405.
[33] Alberio T, Pieroni L, Ronci M, Banfi C, Bongarzone I, Bottoni P, et al. Toward the standardization of mitochondrial proteomics: the Italian mitochondrial human proteome project initiative. J Proteome Res 2017;16:4319–29.
[34] Caterino M, Ruoppolo M, Mandola A, Costanzo M, Orrù S, Imperlini E. Protein-protein interaction networks as a new perspective to evaluate distinct functional roles of voltage-dependent anion channel isoforms. Mol Biosyst 2017;13:2466–76.
[35] Soni V, Upadhayay S, Suryadevara P, Samla G, Singh A, Yogeeswari P, et al. Depletion of *M.tuberculosis* GlmU from infected murine lungs effects the clearance of the pathogen. PLoS Pathog 2015;11:e1005235.
[36] Parikh A, Kumar D, Chawla Y, Kurthkoti K, Khan S, Varshney U, et al. Development of a new generation of vectors for gene expression, gene replacement, and protein-protein interaction studies in mycobacteria. Appl Environ Microbiol 2013;79:1718–29.
[37] Jain P, Hsu T, Arai M, Biermann K, Thaler DS, Nguyen A, et al. Specialized transduction designed for precise high-throughput unmarked deletions in Mycobacterium tuberculosis. mBio 2014;5. e01245-14.
[38] Pandey AK, Raman S, Proff R, Joshi S, Kang CM, Rubin EJ, et al. Nitrile-inducible gene expression in mycobacteria. Tuberculosis (Edinb). 2009;89:12–6.
[39] Caterino M, Ruoppolo M, Fulcoli G, Huynth T, Orrù S, Baldini A, et al. Transcription factor TBX1 overexpression induces downregulation of proteins involved in retinoic acid metabolism: a comparative proteomic analysis. J Proteome Res 2009;8:1515–26.
[40] Arita-Morioka K, Yamanaka K, Mizunoe Y, Ogura T, Sugimoto S. Novel strategy for biofilm inhibition by using small molecules targeting molecular chaperone DnaK. Antimicrob Agents Chemother 2015;59:633–41.
[41] Ojha A, Anand M, Bhatt A, Kremer L, Jacobs Jr WR, Hatfull GF. GroEL1: a dedicated chaperone involved in mycolic acid biosynthesis during biofilm formation in mycobacteria. Cell 2005;123:861–73.
[42] Jiao X, Sherman BT, Stephens R, Baseler MW, Lane HC, Lempicki RA. DAVID-WS: a stateful web service to facilitate gene/protein list analysis. Bioinformatics 2012;28:1805–6.
[43] Itoh Y, Wang X, Hinnebusch BJ, Preston 3rd JF, Romeo T. Depolymerization of beta-1,6-N-acetyl-D-glucosamine disrupts the integrity of diverse bacterial biofilm. J Bacteriol 2005;187:382–7.
[44] Lessard IA, Walsh CT. VanX, a bacterial D-alanyl-D-alanine dipeptidase: resistance, immunity, or survival function? Proc Natl Acad Sci U S A 1999;96:11028–32.
[45] Klotzsche M, Ehrt S, Schnappinger D. Improved tetracycline repressors for gene silencing in mycobacteria. Nucleic Acids Res 2009;37:1778–88.
[46] Pompeo F, van Heijenhoort J, Mengin-Lecreulx D. Probing the role of cysteine residues in glucosamine-1-phosphate acetyltransferase activity of the bifunctional glmu protein from *Escherichia coli*: site-directed mutagenesis and characterization of the mutant enzymes. J Bacteriol 1998;180:4799–803.
[47] Zhang Z, Bulloch EMM, Bunker RD, Baker EN, Squire CJ. Structure and function of GlmU from *Mycobacterium tuberculosis*. Acta Crystallogr D Biol Crystallogr 2009;65:275–83.
[48] Mengin-Lecreulx D, van Heijenoort J. J Bacteriol 1993;175:6150–7.
[49] Buurman ET, Andrews B, Gao N, Hu J, Keating TA, Lahiri S, et al. In vitro validation of acetyltransferase activity of GlmU as an antibacterial target in Haemophilus influenzae. J Boil Chem 2011;286:40734–42.
[50] Stokes SS, Albert R, Buurman ET, Andrews B, Shapiro AB, Green M, et al. Inhibitors of the acetyltransferase domain of N-acetylglucosamine-1-phosphate-uridylyltransferase/glucosamine-1-phosphate-acetyltransferase (GlmU). Part 2: optimization of physical properties leading to antibacterial aryl sulfonamides. Bioorg Med Chem Lett 2012;22:1510–9.
[51] Sharma R, Rani C, Mehra R, Nargotra A, Chib R, Rajput VS, et al. Identification and characterization of novel small molecule inhibitors of the acetyltransferase activity of Escherichia coli N-acetylglucosamine-1-phosphate-uridyltransferase/glucosamine-1-phosphate acetyltransferase (GlmU). Appl Microbiol Biotechnol 2016;100:3071–85.
[52] Singh VK, Syring M, Singh A, Singhal K, Dalecki A, Johansson T. An insight into the significance of the DnaK heat shock system in Staphylococcus aureus. Int J Med Microbiol 2012;302:242–52.
[53] Yeom J, Lee Y, Park W. Effects of non-ionic solute stresses on biofilm formation and lipopolysaccharide production in Escherichia coli O157: H7. Res Microbiol 2012;163:258–67.
[54] Trappetti C, Kadioglu A, Carter M, Hayre J, Iannelli F, Pozzi G, et al. Sialic acid: a preventable signal for pneumococcal biofilm formation, colonization, and invasion of the host. J Infect Dis 2009;199:1497–505.
[55] Sohanpal BK, El-Labany S, Lahooti M, Plumbridge JA, Blomfield IC. Integrated regulatory responses of fimB to N-acetylneuraminic (sialic) acid and GlcNAc in Escherichia coli K-12. Proc Natl Acad Sci USA 2004;101:16322–7.
[56] Jurcisek J, Greiner L, Watanabe H, Zaleski A, Apicella MA, Bakaletz LO. Role of sialic acid and complex carbohydrate biosynthesis in biofilm formation by nontypeable Haemophilus influenzae in the chinchilla middle ear. Infect Immun 2005;73:3210–8.